



Automated calcium scores collected during myocardial perfusion imaging improve identification of obstructive coronary artery disease [☆]



Mirthe Dekker ^{a,b,1,*}, Farahnaz Waissi ^{a,b,1}, Ingrid E.M. Bank ^c, Nikolas Lessmann ^d, Ivana Išgum ^d, Birgitta K. Velthuis ^e, Asbjørn M. Scholtens ^f, Geert E. Leenders ^g, Gerard Pasterkamp ^h, Dominique P.V. de Kleijn ^{a,i}, Leo Timmers ^{c,g}, Arend Mosterd ^j

^a Department of Vascular Surgery, University Medical Center Utrecht, Heidelberglaan 100, 3584 CX Utrecht, the Netherlands

^b Department of Cardiology, Amsterdam University Medical Center, Meibergdreef 9, 1105 AZ Amsterdam, the Netherlands

^c Department of Cardiology, St. Antonius Hospital, Koekoekslaan 1, 3435 CM Nieuwegein, the Netherlands

^d Image Sciences Institute, University Medical Center Utrecht, the Netherlands

^e Department of Radiology, University Medical Center Utrecht, the Netherlands

^f Department of Nuclear Medicine, Meander Medical Center, the Netherlands

^g Department of Cardiology, University Medical Center Utrecht, the Netherlands

^h Department of Clinical Chemistry and Hematology, University Medical Center Utrecht, the Netherlands

ⁱ Netherlands Heart Institute, Moreelsepark 1, 3511 EP Utrecht, the Netherlands

^j Department of Cardiology, Meander Medical Center, Maatweg 3, 3813 TZ Amersfoort, the Netherlands

ARTICLE INFO

Article history:

Received 1 August 2019

Received in revised form 16 October 2019

Accepted 18 October 2019

Available online 19 November 2019

Keywords:

Coronary artery calcium
Obstructive coronary artery disease
Myocardial perfusion imaging
Deep learning
Cardiovascular imaging

ABSTRACT

Background: Myocardial perfusion imaging (MPI) is an accurate noninvasive test for patients with suspected obstructive coronary artery disease (CAD) and coronary artery calcium (CAC) score is known to be a powerful predictor of cardiovascular events. Collection of CAC scores simultaneously with MPI is unexplored.

Aim: We aimed to investigate whether automatically derived CAC scores during myocardial perfusion imaging would further improve the diagnostic accuracy of MPI to detect obstructive CAD.

Methods: We analyzed 150 consecutive patients without a history of coronary revascularization with suspected obstructive CAD who were referred for 82Rb PET/CT and available coronary angiographic data. Myocardial perfusion was evaluated both semi quantitatively as well as quantitatively according to the European guidelines. CAC scores were automatically derived from the low-dose attenuation correction CT scans using previously developed software based on deep learning. Obstructive CAD was defined as stenosis >70% (or >50% in the left main coronary artery) and/or fractional flow reserve (FFR) ≤0.80.

Results: In total 58% of patients had obstructive CAD of which seventy-four percent were male. Addition of CAC scores to MPI and clinical predictors significantly improved the diagnostic accuracy of MPI to detect obstructive CAD. The area under the curve (AUC) increased from 0.87 to 0.91 (p: 0.025). Sensitivity and specificity analysis showed an incremental decrease in false negative tests with our MPI + CAC approach (n = 14 to n = 4), as a consequence an increase in false positive tests was seen (n = 11 to n = 28).

Conclusion: CAC scores collected simultaneously with MPI improve the detection of obstructive coronary artery disease in patients without a history of coronary revascularization.

© 2019 Published by Elsevier B.V. This is an open access article under the CC BY-NC-ND license (<http://creativecommons.org/licenses/by-nc-nd/4.0/>).

Abbreviations: AP, Angina pectoris; AUC, Area under the curve; CABG, Coronary artery bypass grafting; CAC, Coronary artery calcium; CAD, Coronary artery disease; CAG, Coronary angiography; CFR, Coronary flow reserve; CI, Confidence interval; CVD, Cardiovascular disease; FFR, Fractional flow reserve; MBF, Myocardial blood flow; MI, myocardial infarction; MPI, Myocardial perfusion imaging; NPV, Negative predictive value; OR, Odds ratio; PET/CT, Positron emission tomography/computed tomography; PCI, Percutaneous coronary intervention; PPV, Positive predictive value; QCA, Quantitative coronary angiography; ROC, Receiver operator characteristic; SD, Standard deviation; SDS, Summed difference score; WMA, Wall motion abnormalities.

[☆] All of the authors take full responsibility for all aspects of the reliability and freedom from bias of the data presented and their discussed interpretation.

* Corresponding author at: Department of Cardiology, UMC Utrecht, Heidelberglaan 100, PO Box: Q05.2.314, 3508 GA Utrecht, the Netherlands.

E-mail addresses: m.dekker-17@umctrecht.nl (M. Dekker).

¹ Both authors equally contributed to this manuscript.

<https://doi.org/10.1016/j.ijcha.2019.100434>

2352-9067/© 2019 Published by Elsevier B.V.

This is an open access article under the CC BY-NC-ND license (<http://creativecommons.org/licenses/by-nc-nd/4.0/>).

1. Introduction

Angina pectoris (AP) is a clinical syndrome characterized by episodes of retrosternal complaints, usually induced by exercise or other stress factors with quick relieve after discontinuation of exercise or stress. AP is often caused by myocardial ischemia due to the presence of obstructive coronary artery disease (CAD) and/or microvascular dysfunction [1,2]. The diagnostic assessment of patients with suspected obstructive CAD is challenging and one of the most common aspects of cardiology nowadays. Since the presence of obstructive CAD often requires coronary intervention, accurate diagnostic tests are of great importance.

Myocardial perfusion imaging (MPI) with positron emission tomography (PET)/computed tomography (CT) is an accurate non-invasive test for patients with suspected obstructive CAD [3,4]. It provides measurements on myocardial perfusion, myocardial blood flow (MBF) and coronary flow reserve (CFR). The coronary artery calcium (CAC) score on the other hand is a powerful predictor for cardiovascular events [5–9]. Recent studies have demonstrated additional diagnostic power of the CAC score on top of perfusion imaging in patients with suspected obstructive CAD [10–13]. For these studies an additional ECG triggered CT-scan was acquired for manual assessment of CAC scores instead of using the attenuation correction CT images gathered during MPI. Several studies compared manual CAC scoring on an ECG triggered CT with manual CAC scoring on attenuation correction CT images and showed encouraging results [14–16]. Recently, two studies performed in our center compared manual CAC scoring on ECG triggered CT images with automated CAC scoring in low dose chest CT and attenuation correction CT [17,18]. Both studies used a previously developed algorithm based on deep learning and showed that this is a reliable and accurate method of calculating the CAC score.

Therefore, the aim of our study is to assess whether automatically derived CAC scores simultaneously collected with MPI on attenuation correction CT images improve the diagnostic accuracy of MPI in patients with suspected obstructive CAD.

2. Materials and methods

2.1. Study population

The MYOMARKER (MYOcardial ischaemia detection by circulating bioMARKERs) study is a prospective single-center observational cohort study of consecutively enrolled patients (>18 years of age) with suspected CAD who presented at the outpatient clinic of the Meander Medical Center (Amersfoort, the Netherlands) between August 2014 and September 2016. All patients underwent a Rubidium-82 PET/CT scan as part of their diagnostic work-up.

The complete cohort consists of 1265 patients. For the purpose of this study only patients who underwent coronary angiography (CAG) within 90 days prior to or after MPI were selected. After exclusion of patients with previous coronary artery bypass grafting (CABG) or previous percutaneous coronary intervention (PCI), and exclusion of five patients with incomplete MPI results, the final cohort consisted of 150 patients (Appendix A, Fig. A1). The study was approved by the regional medical ethics committee and performed in accordance with the Declaration of Helsinki. Written informed consent was obtained from all participants.

2.2. PET-CT imaging

A detailed description of MPI imaging protocol is provided in the supplemental materials (Appendix B). Briefly, patients were asked to discontinue caffeine- or methylxanthine-containing

food/drinks and theophylline and dipyridamol 48 h prior to the PET/CT scan. Rubidium-82 PET/CT scans were acquired using a hybrid scanner (Biograph CT Flow 64-slice scanner, Siemens Healthcare, Knoxville, Tennessee). Rest and stress cardiac PET/CT images were acquired on the same day, pharmacological stress was administered intravenously with regadenoson. The estimated effective radiation dose for this protocol to the patients was 3.7 mSv. Heart rate, systolic blood pressure and 12 lead ECG were recorded at baseline, 1 min after regadenoson administration and after imaging. Rate-pressure product was calculated for manual correction of rest flow values.

2.3. PET image analysis

Myocardial perfusion was evaluated according to the European guideline in two ways: semi-quantitative and quantitative [19]. All scans were evaluated by 2 experienced observers. Semi-quantitative analysis was performed with the use of the 17-segment model of the American Heart Association [20], in short; the summed difference score (SDS) is the difference between the perfusion deficit score in stress and rest, a SDS score ≥ 4 was defined as stress induced ischemia. Quantitative analysis of myocardial perfusion was assessed by the myocardial blood flow (MBF, mL/g/min) and coronary flow reserve (CFR). MBF was computed from the dynamic rest and stress imaging series with commercially available software (Siemens Syngo Dynamic PET). A global MBF was calculated for the left ventricle as well as regional MBF for each of the three coronary vessel territories. Resting MBF was manually adjusted for the patient-specific rate-pressure product at rest. Global and regional coronary flow reserve was defined as the ratio of hyperemic to (adjusted) baseline MBF.

MPI scans were considered as normal if a patient had a normal MBF, CFR and a SDS score of 0. Normal MBF refers to normal MBF at a threshold of 2.0 ml/g/min. Normal CFR was set 1.6. MPI Scans were considered as suspect for obstructive CAD if either an SDS score Stress ≥ 4 was measured, or patients with an SDS between one and three but with abnormal MBF and/or wall motion abnormalities (WMA).

2.4. Calcium scoring

CAC scores were determined from the low-dose attenuation correction CT scan, which were derived during MPI using a previously developed algorithm [17]. This software was originally developed for fully automated calcium scoring in low dose chest CT scans. We therefore manually annotated coronary calcifications in 200 consecutive CT scans from the present study and retrained the software with a combination of low dose chest CT and low dose attenuation correction CT scans. Briefly the software first detects the lungs to identify a region of interest in the image and then automatically detects CAC above the standard threshold of 130 Hounsfield Units using a deep learning approach. Detected calcifications are labeled according to the affected coronary vessel (left anterior descending including left main coronary artery, left circumflex artery and right coronary artery). CAC scores were calculated for all three coronary vessels [21]. Since this new method is not able to distinguish previously placed coronary stents from coronary calcium we excluded patients with coronary stents from the analysis. CAC scores were categorized according to previous literature as 0, 1–100, 101–300 and 301 or more [5,22].

2.5. Coronary angiography

All lesions were measured by quantitative coronary angiography (QCA) by a blinded trained clinical physician (MD), using Cardiovascular Angiography Analysis System software (CAAS 7.3, Pie

Medical Imaging, Maastricht, The Netherlands). In case of uncertainty a board certified interventional cardiologist (GL) was asked to measure the lesion as a second observer. Uncertainty was mostly based on doubts regarding the second frame in which the lesions should be measured. Lesions were considered hemodynamically important if: 1. FFR positive ≤ 0.80 or 2. A luminal stenosis $>70\%$ (or $>50\%$ in case of left main) measured with QCA. In case of discrepancy between FFR measurement and QCA measurement, FFR result was considered more reliable and therefore used. In total, 15 lesions were measured with FFR.

2.6. Statistical analysis

Continuous data are expressed as mean \pm standard deviation (SD), categorical data as frequencies and percentages. Differences in continuous variables were compared by independent *t*-test. Dichotomous variables were compared by Fisher's exact test. Univariable and multivariable logistic regression were used to analyze predictors for the presence of obstructive CAD. Univariable logistic regression was performed for all variables that were considered possible clinical predictors based on previous literature or differences in baseline characteristics. All variables with a *P* value <0.20 in the univariable analysis were used for the multivariable logistic regression. We used the likelihood ratio test statistic with a backward stepwise method to determine which combination of

clinical predictors performed best in prediction of obstructive CAD. This resulted in the first of three models used for the final analysis. The other two models were derived to compare the diagnostic accuracy of MPI alone versus MPI in combination with automated CAC scores on top of clinical predictors. Benjamini-Hochberg test was used to correct for multiple comparison testing.

The natural logarithm of the CAC score (\ln_CAC+1) was used because of a wide range and right skewness of the CAC scores. Receiver operator characteristic (ROC) areas under the curve (AUC) were calculated for all three models to determine their ability to predict obstructive CAD. We calculated sensitivity, specificity and predictive values for MPI only, CAC scores only and the combination of both. For this analysis ischemia was analyzed as a dichotomized variable. For the CAC score a cut off value of 300 was used since this was considered clinically relevant [6]. All hypotheses tests were two-sided with a critical significance level of <0.05 . Statistical analysis were performed with SPSS version 25.0 (SPSS, Chicago, IL) and R software (R software, version 3.4.1).

3. Results

3.1. Clinical patient characteristics

Clinical characteristics are shown in Table 1. The mean age was 68 ± 12 years, and the majority of patients was male (64%). Patients

Table 1
Clinical characteristics of all patients with and without obstructive CAD.

	All N = 150	No obstructive CAD N = 63	Obstructive CAD N = 87	P value*
Demographics				
Age in years	67.6 (11.5)	66 (10.39)	68 (12.23)	0.470
Male sex	96 (64%)	29 (48%)	67 (74%)	0.001
BMI	28.1 (5.4)	28.7 (6.3)	26.9 (4.6)	0.291
Medical history				
History of CVD	111 (74%)	41 (68%)	70 (78%)	0.196
History of CAD	25 (17%)	3 (5%)	22 (24%)	0.002
History of MI	18 (12%)	2 (3%)	16 (18%)	0.008
History of PAD	10 (7%)	3 (5%)	7 (8%)	0.504
Diabetes mellitus	35 (23%)	14 (23%)	21 (23%)	0.575
Hypertension	97 (65%)	36 (60%)	61 (68%)	0.329
Dyslipidemia	87 (58%)	37 (62%)	50 (56%)	0.458
Current smoker	39 (26%)	15 (25%)	24 (27%)	0.820
Family history of CAD	45 (30%)	19 (32%)	26 (30%)	0.783
Medication				
Platelet aggregation inhibitors†	85 (57%)	29 (48%)	56 (62%)	0.093
Anticoagulants	30 (20%)	11 (18%)	19 (21%)	0.667
Beta-blockers	81 (54%)	31 (52%)	50 (56%)	0.640
Statins	87 (58%)	37 (62%)	50 (56%)	0.458
ACE inhibitor or ARB	57 (38%)	19 (32%)	38 (42%)	0.192
Calcium channel blockers	34 (23%)	16 (27%)	18 (20%)	0.339
Loopdiuretics	22 (15%)	9 (15%)	13 (14%)	0.925
Nitroglycerin	57 (38%)	22 (37%)	35 (39%)	0.784
⁸²Rb PET-CT findings				
Rest LVEF	58 (16)	61 (17)	57 (16)	0.670
Stress LVEF	61 (17)	61 (17)	69 (16)	0.947
SDS	4 (5)	1 (2)	6 (4)	<0.001
RPP	11,024 (3068)	10,341 (2258)	11,501 (3458)	0.227
Rest MBF uncorrected	1.15 (0.38)	1.12 (0.33)	1.17 (0.42)	0.511
Rest MBF corrected	0.86 (0.25)	0.89 (0.24)	0.83 (0.25)	0.170
Stress MBF	2.41 (1.88)	2.61 (0.77)	2.28 (2.35)	0.313
CFR	3.19 (0.99)	3 (1)	3 (1)	0.584
CAC results				
0	8 (5%)	5 (8%)	3 (3%)	0.038
1–100	27 (18%)	17 (27%)	10 (12%)	0.007
101–300	26 (17%)	14 (22%)	12 (14%)	0.043
>300	89 (59%)	27 (43%)	62 (71%)	<0.001

Continuous variables are presented as mean (SD), categorical variables as n(%). * *P* value for comparison between groups with and without obstructive CAD. CVD = cardiovascular disease, CAD = coronary artery disease, MI = myocardial infarction, PAD = peripheral artery disease. †Aspirin, clopidogrel or ticagrelor, LVEF = Left ventricular ejection fraction. SDS = Summed Difference Score [15], RPP = rate pressure product, MBF = myocardial bloodflow, CFR = Coronary flow reserve, CAC = Coronary Artery Calcium.

Table 2
Odds ratios calculated with logistic regression comparing diagnostic performance of MPI and CAC score.

Predictor	Model 1 Clinical predictors		Model 2 Model 1 + MPI		Model 3 Model 2 + CAC score	
	OR (95% CI)	P value	OR (95% CI)	P value	OR (95% CI)	P value
Male sex	2.94 (1.44–6.12)	0.003	2.33 (0.91–6.0)	0.078	1.90 (0.70–5.11)	0.212
History of CAD	5.70 (1.60–20.46)	0.008	11.0 (2.35–51.53)	0.002	10.75 (2.05–56.53)	0.005
Ischemia	–	–	27.7 (10.60–72.26)	<0.001	26.49 (9.45–74.24)	<0.001
Ln_CAC	–	–	–	–	2.47 (1.40–4.34)	0.002

MPI = myocardial perfusion imaging, CAC score = coronary artery calcium score, Ischemia = dichotomized with a cut off SDS score of 4 and/or abnormal myocardial blood-flow/coronary flowreserve, Ln_CAC = natural logarithm of coronary artery calcium score + 1.

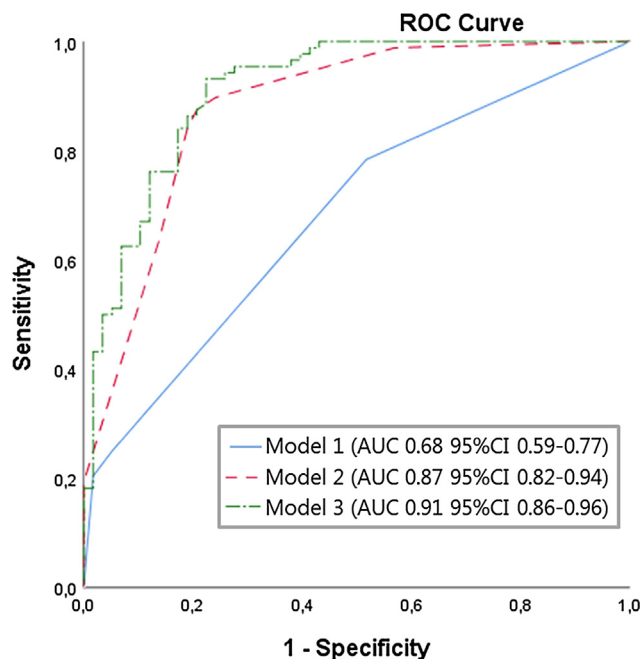


Fig. 1. ROC Curves diagnostic models. ROC Curves with corresponding AUC values for all three models in complete cohort. Model 1 contains the clinical predictors, in model 2 the presence of ischemia is added, the third model consist of the clinical predictors, presence of ischemia and the CAC score. P value for difference in AUC between model 2 and 3 was 0.025.

had a mean BMI of 28.1 kg/m². Already 57% of the patients were using platelet aggregation inhibition (aspirin, clopidogrel or ticagrelor) in accordance with their previous medical history of atherosclerotic disease. Patients with obstructive CAD were more often male (74% vs. 48%, p value 0.001), and had more often a history of CAD (24% vs. 5%, p value 0.002) or previous myocardial infarction (18% vs. 3%, p value 0.008). There were no differences in age, BMI, or any of the other known risk factors for cardiovascular disease between patients with and without obstructive CAD. The left ventricular ejection fraction was above normal limit during stress and rest in all patients. As expected, the average SDS score in patients with obstructive CAD was higher compared to those

Table 3
Estimated diagnostic performance to predict obstructive CAD in clinical practice.

Measure	TP	TN	FP	FN	Sensitivity	Specificity	PPV	NPV	AUC (95%CI)
Ischemia*	76	49	11	14	0.84	0.82	0.87	0.78	0.83 (0.76–0.90)
CAC score†	67	38	22	23	0.74	0.63	0.75	0.62	0.69 (0.60–0.78)
Ischemia_CAC score‡	86	32	28	4	0.96	0.53	0.75	0.89	0.74 (0.66–0.83)

TP = True positive, TN = True negative, FP = False positive, FN = False negative, PPV = Positive Predictive value, NPV = Negative predictive value, *Ischemia = dichotomized with a cut off SDS score of 4 and/or abnormal myocardial bloodflow/coronary flowreserve, †CAC score = coronary artery calcium score as dichotomous variable, <300 or >300. ‡Ischemia_CAC = dichotomized as either ischemia and/or CAC score >300.

without (6 vs. 1, p value <0.001). No difference between (un)corrected rest MBF, hyperemic MBF and CFR were observed. There were in total 8 patients with a CAC score of 0. In patients with obstructive CAD the majority of patients had CAC scores >300 (71%).

3.2. Predictors of obstructive CAD

In the univariable analysis (Appendix C, Table C1) male sex (OR 3.11, 95% CI 1.56–6.23), history of cardiovascular disease (CVD) (OR 1.62, 95%CI 0.78–3.39), history of CAD (OR 6.15, 95% CI 1.75–21.60), previous myocardial infarction (MI) (OR 6.27, 95% CI 1.39–28.37), use of an ACE-inhibitor and/or ARB (OR 1.58, 95% CI 0.80–3.13) and use of a platelet aggregation inhibitor (OR 1.76, 95% CI 0.91–3.41) were considered as significant clinical predictors of obstructive CAD. These variables were used for multivariable analysis, finally after model reduction with the likelihood ratio test male sex and history of CAD remained significant predictors of obstructive CAD.

3.3. Diagnostic performance of combined models

Table 2 shows the final three constructed models. The first model contains the clinical predictors (male sex and history of CAD) for the presence of obstructive CAD selected with multivariable logistic regression. In the second model the presence of ischemia on MPI (SDS ≥ 4, or SDS 1–3 and abnormal MBF/WMA) was added to the first the model. CFR was considered as possible MPI-derived predictor for the presence of obstructive CAD, but it showed no additive effect on the model performance (OR 1.10 95%CI 0.78–1.58 p value 0.501 appendix C1). In the third model, CAC score was added on top of the second model. Both the presence of ischemia on MPI (OR 26.49, 95%CI 9.45–74.24) and the CAC score (OR 2.47, 95%CI 1.40–4.34) were significant predictors for the presence of obstructive CAD in addition to the clinical predictors. Corresponding ROC curves with AUC values are shown in Fig. 1. The diagnostic accuracy of MPI to detect obstructive CAD improved with 4% when adding the automatically derived CAC scores (0.87 vs. 0.91). This difference in AUC between model 2 and 3 was statistically significant, p value 0.025.

Table 3 provides an overview of the estimated diagnostic parameters in clinical practice for three single parameters

comparing the use of the presence of ischemia alone, CAC scores (dichotomized as either <300 or >300) alone and presence of ischemia and/or a CAC scores above 300. When comparing MPI result on its own (AUC 0.83, 95%CI 0.76–0.90) with only CAC scores (AUC 0.69, 95% CI 0.60–0.78), both sensitivity (0.84 vs. 0.74) and specificity (0.82 vs. 0.63) were better in the model with only MPI, according to existing literature. Addition of CAC scores to MPI data substantially reduced the number of false negative tests (from $n = 14$ to $n = 4$ patients), which leads to a remarkable increase of the sensitivity and negative predictive value. As a consequence, the number of false positive tests is increased (from $n = 11$ to $n = 28$), which affects the specificity and positive predictive value of the tests.

4. Discussion

This study was a proof-of-concept to see whether our algorithm could automatically determine CAC scores on low-dose CT images gathered during MPI. We showed that presence of ischemia and CAC scores were both significant predictors of obstructive CAD in addition to clinical parameters. We have shown that addition of these CAC scores increased the diagnostic accuracy of MPI to detect obstructive CAD (AUC increase 4%, p value for difference 0.025). The increased diagnostic yield is mainly due to the reduction of false negative test results ($N = 14$ to $N = 4$). Important counterpart to this finding was the increased number of false positive tests ($N = 11$ to $N = 28$), this needs further research.

4.1. Predictors of obstructive coronary artery disease

In line with previous studies, history of CAD, ischemia and the CAC score were significant predictors for the presence of obstructive CAD [3,5,7,9]. In contrast, none of the generally accepted risk factors (smoking, diabetes, hypertension and dyslipidemia) for obstructive CAD were significant predictors in our population [2]. This might be the result of our high risk study population, namely only patients referred for CAG were included. The same is seen in previous comparable studies [12,13].

In our results CFR did not contribute to the prediction of the presence of obstructive CAD (OR 1.10 95%CI 0.78–1.58). Several studies established an association between low CFR and adverse cardiac outcomes [23–26]. However, they did not use CFR as a predictor of obstructive CAD. Taqueti et al. showed that impaired CFR is not only a marker of epicardial disease but especially a marker of diffuse nonobstructive CAD and microvascular dysfunction [27]. They state that CFR might be especially useful in women and diabetic patients. The limited added diagnostic value of CFR in our study was therefore not surprising.

4.2. Diagnostic performance of MPI and automated CAC score

Diagnostic performance of MPI and automated CAC score alone were in agreement with previous literature [2]. Existing literature on the added value of CAC scoring in addition to MPI is limited. Bybee et al. analyzed patients with a negative MPI and found sub-clinical atherosclerosis in 22–30% of the patients with the use of CAC scores [28]. Thompson et al. showed 17% reclassification of patients with normal MPI results into having obstructive CAD after adding CAC scores [29]. Schepis et al. observed the added value of CAC scores in patients with suspected obstructive CAD [11]. They showed an increased sensitivity of MPI after adding CAC scores from 76% to 83%. In our study an even larger beneficial effect was observed (increase of 84% to 96%). Zampella et al. showed an AUC of a combined model with CAC score and MPI (without clinical parameters) of 0.79 [13]. Regardless of our much more heteroge-

neous population we showed similar results (AUC combined model 0.74, 95% CI 0.66–0.83). Danad et al. showed that the incremental value of a combined assessment of PET with coronary CT also depends on which nuclear tracer is used [30]. An important difference between existing literature and our study is the use of a fully automated CAC scoring algorithm, which makes acquisition of extra CT-images and manual scoring unnecessary. These results are therefore more directly applicable in clinical practice because only already available information from PET/CT is used. The clear benefit of our method is the reduction in false negative test results, since this would be of great importance for patientcare. However, the overall performance of our combined model showed slight reduction of diagnostic performance compared to a model with only MPI (AUC 0.74 vs 0.83). This is due to the increased number of false positive test results leading to poor specificity. Special caution for the interpretation of a newly positive tests results after addition of CAC scores is therefore necessary. Future research should focus on this.

4.3. Strengths and limitations

This study was a single center retrospective analysis on perfusion imaging data. Patients with a previous CABG were excluded because MPI often yields positive results just above the level of the anastomosis and correlation with epicardial coronary artery disease is notoriously complicated in post CABG patients. We did not use core lab evaluations for the coronary angiography results, however we did perform QCA analysis on all lesions. As in all MPI studies with CAG as reference, there will be referral bias. We observed an increase of false positive tests as a result of the decrease in false negative test results, which has an impact on the specificity. Most patients with negative tests results are not referred for angiography, this might have induced biased assessment of the true negative fraction. However future studies should focus on reducing the amount of false positive test results to make this method trustworthy in clinical practice.

There are several strengths of this study. This is real world data from a center with high numbers of rubidium PET imaging. To our knowledge this is the largest study on the simultaneous assessment of ischemia and CAC scores on MPI images for the detection of obstructive CAD. Another important strength is the algorithm which is used to calculate the CAC scores which is fully automated and easily applicable to data that is already acquired for another purpose. Currently this software is not (yet) free available, however it is possible to purchase a license and use the algorithm.

5. Conclusion

We found that automatically derived coronary calcium scores simultaneously collected with MPI improve the diagnostic accuracy of MPI for the detection of obstructive CAD in patients with suspected myocardial ischemia without previous coronary revascularization.

6. Disclosures

None of the authors had a relationships with the industry to declare.

Funding

This work was supported by the Dutch Heart Foundation, CVON 2017-05 PERSUASIVE.

Acknowledgements

None.

Supplementary data

Supplementary data to this article can be found online at <https://doi.org/10.1016/j.ijcha.2019.100434>.

References

- [1] National Institutes of Health NH, Lung and B.I., *Morbidity & Mortality: 2012 Chart Book on Cardiovascular, Lung, and Blood Diseases*, S. Bethesda, MD Natl. Hear. Lung, Blood Institute, 2012.
- [2] K. Fox, M.A.A. Garcia, D. Ardissino, et al., Task Force on the Management of Stable Angina Pectoris of the European Society of Cardiology, ESC Committee for Practice Guidelines (CPG), Guidelines on the management of stable angina pectoris: executive summary: The Task Force on the Management of Stable Angina Pectoris of the European Society of Cardiology, *Eur. Heart J.* 27 (2006) 1341–1381.
- [3] U.K. Sampson, S. Dorbala, A. Limaye, R. Kwong, M.F. Di Carli, Diagnostic accuracy of rubidium-82 myocardial perfusion imaging with hybrid positron emission tomography/computed tomography in the detection of coronary artery disease, *J. Am. Coll. Cardiol.* 49 (2007) 1052–1058.
- [4] N.P. Johnson, K.L. Gould, Physiological basis for angina and ST-segment change PET-verified thresholds of quantitative stress myocardial perfusion and coronary flow reserve, *J. Am. Coll. Cardiol. Img.* 4 (2011) 990–998.
- [5] R. Detrano, A.D. Guerci, J.J. Carr, et al., Coronary calcium as a predictor of coronary events in four racial or ethnic groups, *N. Engl. J. Med.* 358 (2008) 1336–1345.
- [6] T.S. Polonsky, R.L. McClelland, N.W. Jorgensen, D.E. Bild, G.L. Burke, A.D. Guerci, P. Greenland, Coronary artery calcium score and risk classification for coronary heart disease prediction, *JAMA* 303 (2010) 1610–1616.
- [7] J. Yeboah, R.L. McClelland, T.S. Polonsky, et al., Comparison of novel risk markers for improvement in cardiovascular risk assessment in intermediate-risk individuals, *JAMA* 308 (2012) 788–795.
- [8] S.A.E. Peters, H.M. den Ruijter, M.L. Bots, K.G.M. Moons, Improvements in risk stratification for the occurrence of cardiovascular disease by imaging subclinical atherosclerosis: a systematic review, *Heart* 98 (2012) 177–184.
- [9] R.L. McClelland, N.W. Jorgensen, M. Budoff, et al., 10-Year Coronary Heart Disease Risk Prediction Using Coronary Artery Calcium and Traditional Risk Factors: Derivation in the MESA (Multi-Ethnic Study of Atherosclerosis) With Validation in the HNR (Heinz Nixdorf Recall) Study and the DHS (Dallas Heart Stu), *J. Am. Coll. Cardiol.* 66 (2015) 1643–1653.
- [10] S. Leschka, H. Scheffel, L. Desbiolles, et al., Combining dual-source computed tomography coronary angiography and calcium scoring: added value for the assessment of coronary artery disease, *Heart* 94 (2008) 1154–1161.
- [11] T. Schepis, O. Gaemperli, P. Koepfli, et al., Added value of coronary artery calcium score as an adjunct to gated SPECT for the evaluation of coronary artery disease in an intermediate-risk population, *J. Nucl. Med.* 48 (2007) 1424–1430.
- [12] Y. Brodov, H. Gransar, D. Dey, et al., Combined Quantitative Assessment of Myocardial Perfusion and Coronary Artery Calcium Score by Hybrid 82Rb PET/CT Improves Detection of Coronary Artery Disease, *J. Nucl. Med.* 56 (2015) 1345–1350.
- [13] E. Zampella, W. Acampa, R. Assante, et al., Combined evaluation of regional coronary artery calcium and myocardial perfusion by 82Rb PET/CT in the identification of obstructive coronary artery disease, *Eur. J. Nucl. Med. Mol. Imag.* 45 (2018) 521–529.
- [14] A.J. Einstein, L.L. Johnson, S. Bokhari, J. Son, R.C. Thompson, T.M. Bateman, S.W. Hayes, D.S. Berman, Agreement of visual estimation of coronary artery calcium from low-dose CT attenuation correction scans in hybrid PET/CT and SPECT/CT with standard Agatston score, *J. Am. Coll. Cardiol.* 56 (2010) 1914–1921.
- [15] I. Mylonas, M. Kazmi, L. Fuller, et al., Measuring coronary artery calcification using positron emission tomography-computed tomography attenuation correction images, *Eur. Heart J. Cardiovasc. Imag.* 13 (2012) 786–792.
- [16] T.S. Kaster, G. Dwivedi, L. Susser, J.M. Renaud, R.S.B. Beanlands, B.J.W. Chow, R. A. DeKemp, Single low-dose CT scan optimized for rest-stress PET attenuation correction and quantification of coronary artery calcium, *J. Nucl. Cardiol.* 22 (2015) 419–428.
- [17] N. Lessmann, B. Van Ginneken, M. Zreik, P.A. De Jong, B.D. De Vos, M.A. Viergever, I. Isgum, Automatic Calcium Scoring in Low-Dose Chest CT Using Deep Neural Networks with Dilated Convolutions, *IEEE Trans. Med. Imag.* 37 (2018) 615–625.
- [18] I. Işgum, B.D. de Vos, J.M. Wolterink, D. Dey, D.S. Berman, M. Rubeaux, T. Leiner, P.J. Slomka, Automatic determination of cardiovascular risk by CT attenuation correction maps in Rb-82 PET/CT, *J. Nucl. Cardiol.* 25 (2018) 2133–2142.
- [19] J. Bax, F. Bengel, E.B. Sokole, et al., Guidelines EANM/ESC procedural guidelines for myocardial perfusion imaging in nuclear cardiology, 32 (2005) 855–897.
- [20] M.D. Cerqueira, N.J. Weissman, V. Dilsizian, et al., American Heart Association Writing Group on Myocardial Segmentation and Registration for Cardiac Imaging, Standardized myocardial segmentation and nomenclature for tomographic imaging of the heart. A statement for healthcare professionals from the Cardiac Imaging Committee of the Council on Clinical Cardiology of the American Heart Association, *Int. J. Cardiovasc. Imag.* 18 (2002) 539–542.
- [21] A.S. Agatston, W.R. Janowitz, F.J. Hildner, N.R. Zusmer, M. Viamonte, R. Detrano, Quantification of coronary artery calcium using ultrafast computed tomography, *J. Am. Coll. Cardiol.* 15 (1990) 827–832.
- [22] P. Greenland, L. LaBree, S.P. Azen, T.M. Doherty, R.C. Detrano, Coronary artery calcium score combined with Framingham score for risk prediction in asymptomatic individuals, *JAMA* 291 (2004) 210–215.
- [23] B.A. Herzog, L. Husmann, I. Valenta, et al., Long-term prognostic value of 13N-ammonia myocardial perfusion positron emission tomography added value of coronary flow reserve, *J. Am. Coll. Cardiol.* 54 (2009) 150–156.
- [24] V.L. Murthy, M. Naya, C.R. Foster, et al., Association between coronary vascular dysfunction and cardiac mortality in patients with and without diabetes mellitus, *Circulation* 126 (2012) 1858–1868.
- [25] V.L. Murthy, M. Naya, C.R. Foster, et al., Improved cardiac risk assessment with noninvasive measures of coronary flow reserve, *Circulation* 124 (2011) 2215–2224.
- [26] M.C. Ziadi, R.A. Dekemp, K.A. Williams, et al., Impaired myocardial flow reserve on rubidium-82 positron emission tomography imaging predicts adverse outcomes in patients assessed for myocardial ischemia, *J. Am. Coll. Cardiol.* 58 (2011) 740–748.
- [27] V.R. Taqueti, L.J. Shaw, N.R. Cook, et al., Excess cardiovascular risk in women relative to men referred for coronary angiography is associated with severely impaired coronary flow reserve, not obstructive disease, *Circulation* 135 (2017) 566–577.
- [28] K.A. Bybee, J. Lee, R. Markiewicz, et al., Diagnostic and clinical benefit of combined coronary calcium and perfusion assessment in patients undergoing PET/CT myocardial perfusion stress imaging, *J. Nucl. Cardiol.* 17 (2010) 188–196.
- [29] R.C. Thompson, A.I. McGhie, K.W. Moser, J.H. O'Keefe, T.L. Stevens, J. House, N. Fritsch, T.M. Bateman, Clinical utility of coronary calcium scoring after nonischemic myocardial perfusion imaging, *J. Nucl. Cardiol.* 12 (2005) 392–400.
- [30] I. Danad, P.G. Raijmakers, P. Knaapen, Diagnosing coronary artery disease with hybrid PET/CT: it takes two to tango, *J. Nucl. Cardiol.* 20 (2013) 874–890.